blood®
Plenary Paper

RED CELLS, IRON, AND ERYTHROPOIESIS

Hemolysis in the spleen drives erythrocyte turnover

T. R. L. Klei,[1,2] J. Dalimot,[1] B. Nota,[3] M. Veldthuis,[4] F. P. J. Mul,[3] T. Rademakers,[5] M. Hoogenboezem,[3] S. Q. Nagelkerke,[1] W. F. J. van IJcken,[6] E. Oole,[6] P. Svendsen,[7] S. K. Moestrup,[7,8] F. P. J. van Alphen,[3] A. B. Meijer,[3,9,10] T. W. Kuijpers,[11-13] R. van Zwieten,[1,4] and R. van Bruggen[1]

[1]Department of Blood Cell Research, Sanquin Research and Landsteiner Laboratory, University of Amsterdam, Amsterdam, The Netherlands; [2]Department of Product and Process Development, Sanquin Blood Bank, Amsterdam, The Netherlands; [3]Department of Research Facilities, Sanquin Research and Laboratory Services, Amsterdam, The Netherlands; [4]Laboratory for Red Blood Cell Diagnostics, Sanquin, Amsterdam, The Netherlands; [5]Department of Plasma Proteins, Laboratory for Molecular Cell Biology, Sanquin Research and Landsteiner Laboratory, University of Amsterdam, Amsterdam, The Netherlands; [6]Erasmus Medical Center, University Medical Center Rotterdam, Department of Cell Biology, Center for Biomics, Rotterdam, The Netherlands; [7]Department of Biomedicine, Aarhus University, Aarhus, Denmark; [8]Department of Molecular Medicine University of Southern Denmark, Odense, Denmark; [9]Department of Molecular and Cellular Hemostasis, Sanquin Research and Landsteiner Laboratory, University of Amsterdam, Amsterdam, The Netherlands; [10]Department of Biomolecular Mass Spectrometry and Proteomics, Utrecht Institute for Pharmaceutical Sciences (UIPS), Utrecht University, Utrecht, The Netherlands; [11]Department of Molecular Cell Biology and Immunology, Sanquin Research and Landsteiner Laboratory, University of Amsterdam, Amsterdam, The Netherlands; [12]Vrije Universiteit Medical Center, Amsterdam, The Netherlands; and [13]Emma Children's Hospital, Academic Medical Center, University of Amsterdam, Amsterdam, The Netherlands

KEY POINTS

- **Aged erythrocytes interact with the extracellular matrix of the spleen, resulting in hemolysis and ghost formation.**
- **Ghost formation enables recognition and phagocytosis of senescent erythrocytes by RPMs.**

Red pulp macrophages (RPMs) of the spleen mediate turnover of billions of senescent erythrocytes per day. However, the molecular mechanisms involved in sequestration of senescent erythrocytes, their recognition, and their subsequent degradation by RPMs remain unclear. In this study, we provide evidence that the splenic environment is of substantial importance in facilitating erythrocyte turnover through induction of hemolysis. Upon isolating human spleen RPMs, we noted a substantial lack of macrophages that were in the process of phagocytosing intact erythrocytes. Detailed characterization of erythrocyte and macrophage subpopulations from human spleen tissue led to the identification of erythrocytes that are devoid of hemoglobin, so-called erythrocyte ghosts. By using in vivo imaging and transfusion experiments, we further confirmed that senescent erythrocytes that are retained in the spleen are subject to hemolysis. In addition, we showed that erythrocyte adhesion molecules, which are specifically activated on aged erythrocytes, cause senescent erythrocytes to interact with extracellular matrix proteins that are exposed within the splenic architecture. Such adhesion molecule–driven retention of senescent erythrocytes under low shear conditions was found to result in steady shrinkage of the cell and ultimately resulted in hemolysis. In contrast to intact senescent erythrocytes, the remnant erythrocyte ghost shells were prone to recognition and breakdown by RPMs. These data identify hemolysis as a key event in the turnover of senescent erythrocytes, which alters our current understanding of how erythrocyte degradation is regulated. (*Blood*. 2020;136(14):1579-1589)

Introduction

Erythrocytes circulate for an average of 120 days before becoming prone to removal from the circulation.[1,2] Various processes and factors have been identified that may contribute to sequestration and phagocytosis of senescent erythrocytes. These include accumulation of removal signals such as phosphatidylserine exposure,[2] conformational changes in CD47,[3] oxidation of proteins[4] and lipids that render them susceptible to complement deposition,[5,6] loss of membrane deformability,[7-9] and activation of adhesion molecules.[10,11] These observations can explain why certain genetic diseases that affect erythrocyte membrane deformability, such as sickle cell disease and spherocytosis, result in anemia.

Strikingly, loss of deformability is not always associated with enhanced erythrocyte turnover. An interesting example is southeast Asian ovalocytosis (SAO). SAO is an uncommon hereditary disorder in which the membrane protein Band3 interacts with the underlying cytoskeleton in a stronger than normal manner, resulting in poorly deformed erythrocytes.[12,13] In contrast to sickle cell disease and spherocytosis, SAO is clearly not associated with large-scale erythrocyte destruction.[14] This is one of the reasons why it has been proposed that, next to loss of deformability, other factors may contribute to retention of erythrocytes within the spleen, leading to their turnover. One example is the activation of adhesion molecules such as Lu/BCAM and CD44 specifically on aged erythrocytes.[10,11] It is not yet clear how erythrocyte retention in the spleen is orchestrated.

Next to retention of senescent erythrocytes, their subsequent recognition and phagocytosis by splenic red pulp macrophages (RPMs) is also a process that is not well understood. This is

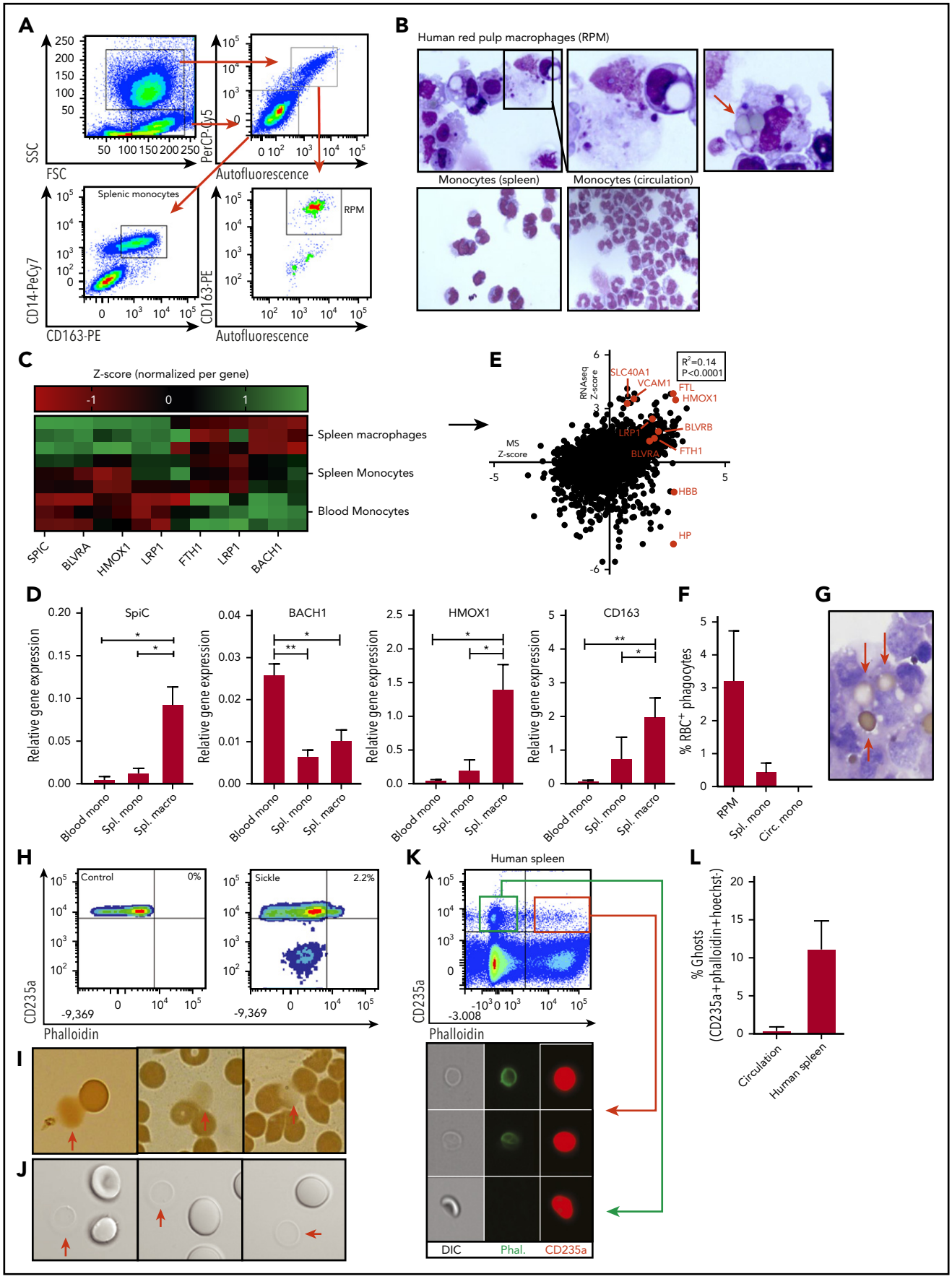
A
SSC
FSC
PerCP-Cy5
Autofluorescence
Splenic monocytes
RPM
CD14-PeCy7
CD163-PE
CD163-PE
Autofluorescence
B
Human red pulp macrophages (RPM)
Monocytes (spleen)
Monocytes (circulation)
C
Z-score (normalized per gene)
Spleen macrophages
Spleen Monocytes
Blood Monocytes
SPIC
BLVRA
HMOX1
LRP1
FTH1
LRP1
BACH1
E
RNAseq Z-score
MS Z-score
R²=0.14
P<0.0001
SLC40A1
VCAM1
FTL
HMOX1
LRP1
BLVRB
BLVRA
FTH1
HBB
HP
D
SpiC
BACH1
HMOX1
CD163
Relative gene expression
Blood mono
Spl. mono
Spl. macro
F
% RBC+ phagocytes
RPM
Spl. mono
Circ. mono
G
H
Control
0%
Sickle
2.2%
CD235a
Phalloidin
-9,369
I
J
K
Human spleen
CD235a
Phalloidin
-3.008
DIC
Phal.
CD235a
L
% Ghosts (CD235a+phalloidin+hoechst-)
Circulation
Human spleen

Figure 1.

exemplified in a mouse study in which physiologically aged erythrocytes were found to undergo phagocytosis by RPMs in vivo but not in vitro.[15] This finding suggested that the splenic architecture may play an important role in facilitating erythrocyte turnover. It was also concluded that studies demonstrating acquisition of specific senescence markers, which may include heat-hardening of red blood cells, opsonization, fixation, or otherwise damaging the erythrocyte, may not be representative for what is occurring during physiological ageing of erythrocytes.

Thus, it is clear that there are many uncertainties regarding the factors that drive turnover of physiologically aged erythrocytes and the impact of the splenic architecture on this process. To gain insight into these processes, we studied RPMs and erythrocytes isolated from human spleen tissue. We found that human spleen tissue is filled with erythrocyte ghosts, the membrane remnants of erythrocytes that have lost their hemoglobin content. By performing in vivo transfusion experiments, we showed that these erythrocyte ghosts form as a consequence of prolonged erythrocyte retention under low shear stresses. In addition, we showed that laminin-α5, the ligand of Lu/BCAM that is specifically activated on aged erythrocytes, is exposed in human spleen tissue. Indeed, the physical interaction between Lu/BCAM and laminin-α5 was found to similarly induce hemolysis. Finally, the remnant erythrocyte ghosts that form as a result of this interaction were readily recognized and phagocytosed by RPMs in vivo and in vitro. These findings thus demonstrate that hemolysis is a key contributor to erythrocyte turnover.

Methods

Blood samples and buffers

Venous blood was obtained in heparinized tubes from healthy volunteers after informed consent. Blood studies were approved by the Medical Ethical Committee of Sanquin Research and performed in accordance with the 2013 Declaration of Helsinki. Erythrocytes were isolated by centrifugation of whole blood at 230*g* for 15 minutes. Next, plasma and buffy coat were removed, and erythrocytes were washed twice with saline-adenine-glucose-mannitol (SAGM) medium (150 mM NaCl, 1.25 mM adenine, 50 mM glucose, 29 mM mannitol [pH 5.6]; Fresenius SE). Erythrocytes were then washed twice in *N*-2-hydroxyethylpiperazine-*N*′-2-ethanesulfonic acid (HEPES) (HEPES+ consists of 132 mM NaCl, 20 mM HEPES, 6 mM KCl, 1 mM $MgSO_4$, 1.2 mM K_2HPO_4, (all from Sigma-Aldrich, St Louis, MO) supplemented with 1 mM Ca^{2+}, 0.5% human serum albumin, and 1 mg/mL glucose. Spleen tissue was obtained from organ transplant donors as rest material for research purposes.

RPM and spleen monocyte isolation

Collagenase buffer containing 100 U/mL collagenase (CLSPA; Worthington, Columbus, OH), 2 Kunitz-type units/mL DNAse (deoxyribonuclease I bovine recombinant; Sigma-Aldrich), 0.5 μg/mL aggrastat (MSD), 1 mg/mL glucose (Sigma-Aldrich), and 1 mM Ca^{2+} in HEPES buffer was injected into a piece of human spleen. The suspension was incubated at 37°C for 30 minutes, followed by filtration over a 100-μm filter to create a single-cell suspension. Subsequently, erythrocytes were lysed by incubating the suspension with isotonic ammonium chloride buffer for 5 minutes at 4°C. RPMs and splenic monocytes were then isolated by the Aria III Cell Sorter (BD Biosciences, Franklin Lakes, NJ) as indicated in Figure 1A.

In vivo transfusion assays and intravital microscopy

The animals were handled according to the guidelines prescribed by Dutch legislation. Female C57BL/6 mice were injected with 2×10^8 fresh erythrocytes or erythrocytes that had been stored for 2 weeks in SAGM storage medium at 4°C, referred to as senescent erythrocytes. Before injection, erythrocytes were stained with PKH26 (1:500, 30 minutes, 37°C) and calcein-AM (1:1000, 30 minutes, 37°C) in HEPES buffer without albumin. Depending on the experiment, mice were euthanized either 2 or 3 hours after transfusion or anesthetized using 2% isoflurane for intravital microscopy purposes. Afterward, the spleen was extra-corporeally immobilized on a silicone frame and immersed in phosphate-buffered saline (PBS) for imaging. To determine haptoglobin and hemopexin concentrations in mouse organs, the organs were harvested, incised, and incubated in 150 μL PBS for 30 minutes in Costar filter spintubes (Sigma-Aldrich). Afterward, plasma was extruded by centrifugation for 5 minutes at 520*g*. Haptoglobin and hemopexin concentrations were determined by enzyme-linked immunosorbent assay (R&D Systems, Minneapolis, MN).

Ghost formation and phagocytosis assays

In a ghost formation plate assay, erythrocytes were allowed to sediment for 30 minutes. after which they were incubated for 3.5 hours at 37°C with shaking at 300 rpm, after which ghost formation was assessed by phalloidin staining using flow cytometry. The plates were either uncoated or coated with fibronectin (CLB, Amsterdam, The Netherlands), collagen (Sigma-Aldrich), hyaluronic acid (Sigma-Aldrich), or laminin-α5 (BioLamina, Sundbyberg, Sweden). For phagocytosis assays, control erythrocytes, senescent erythrocyte CD235a, immunoglobulin G

Figure 1. Characterization of human RPMs and erythrocyte turnover. (A) Flow cytometry gating strategy used to isolate human spleen RPMs and splenic monocytes. Forward scatter and side scatter (SSC) were used to differentiate between monocyte and macrophage-containing populations of cells. From the granulocyte and macrophage-containing gate (left upper panel), the autofluorescent (AF) cells were selected (right upper panel) which were further subdivided into CD163-expressing and -nonexpressing cells (lower right panel). The $CD163^+AF^+$ cells are the RPMs. From the lower forward scatter and side scatter gate, the monocytes were isolated on the basis of CD14 and CD163 expression (lower left panel). (B) Representative cytospin micrograph of flow cytometry-sorted spleen-derived RPMs, splenic monocytes, and circulatory monocytes. (C) *Z* scores of genes related to iron recycling obtained by RNA sequencing (RNA-seq) on RPMs, splenic monocytes, and circulatory monocytes (n = 3). (D) Quantitative polymerase chain reaction was performed to verify RNA-seq data. Gene expression is normalized to the GAPDH housekeeping gene and expressed as relative gene expression (n = 3, mean ± SD). In line with the increased SpiC expression in RPMs, BACH1, the repressor of SpiC, was found to be downregulated. (E) Correlation between relative protein expression as determined by mass spectrometry (MS) (n = 5) and transcript abundance as determined by RNA-seq (n = 3) by RPMs. Several genes of interest are shown in red. (F) Quantification of the percentage of RPMs with ≥1 erythrocyte inclusions as depicted in Figure 1B (n = 3-6). (G) Representative benzidine staining of human RPMs depicting relatively intact adhering and internalized erythrocytes. (H) Ghost erythrocytes were detected by F-actin staining (phalloidin) in combination with antiglycophorin-A staining for the erythroid-specific marker (antiCD235a). (I-J) Conventional light microscope micrograph and benzidine staining depicting erythrocytes and erythrocyte ghosts (red arrows). (K-L) Flow cytometric gating strategy used to quantify ghost erythrocytes in the circulation of healthy individuals and in human spleen tissue. White lines mark border cropping of the image because the output file was too large. $^*P < .05$; $^{**}P < .01$ (mean ± SD). Circ, circulating; macro, macrophage; mono, monocyte; ns, not significant; Spl., spleen.

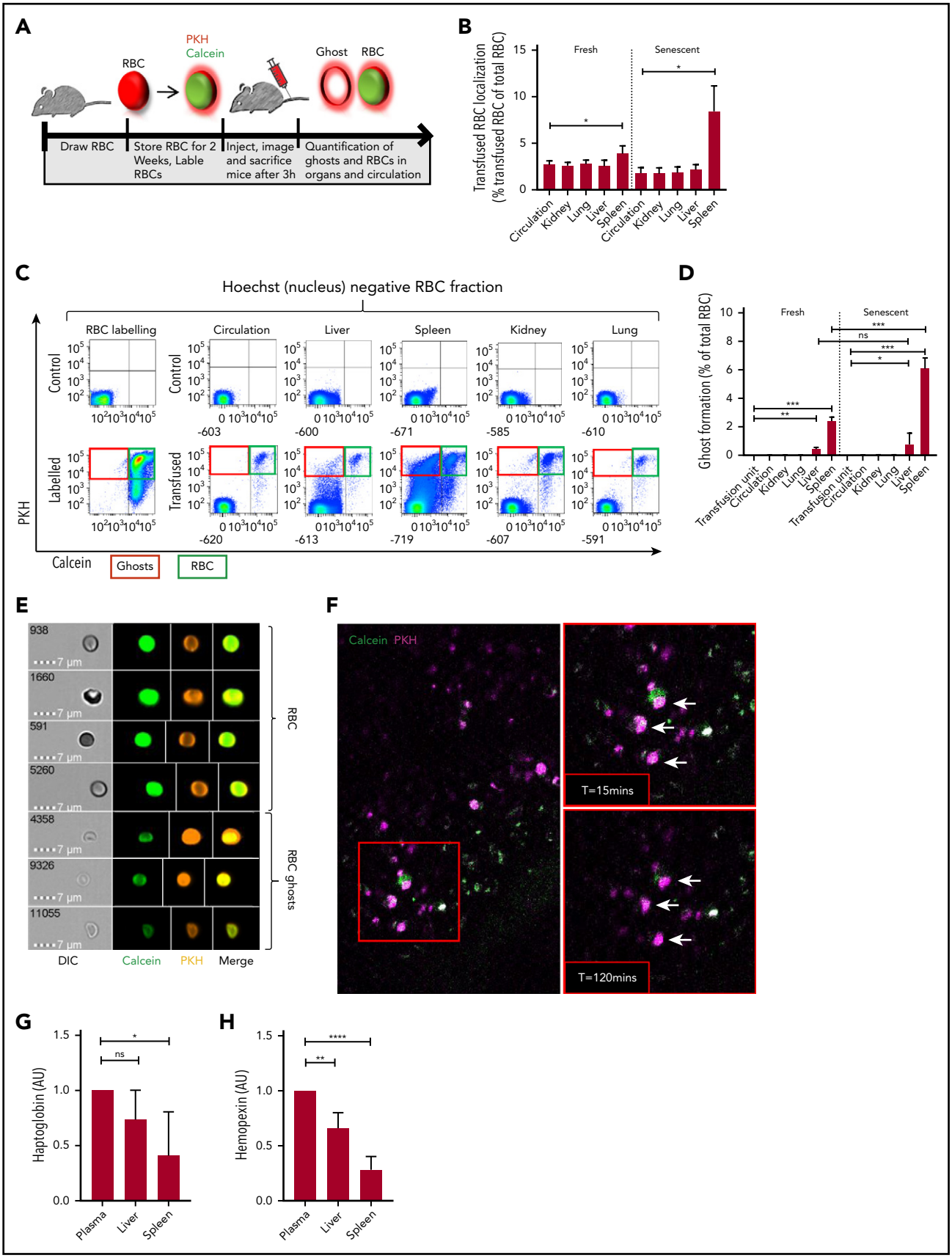

Figure 2. Senescent erythrocytes are prone to hemolysis within the spleen in vivo. (A) Setup used to determine ghost formation in vivo. Mouse erythrocytes were stored in SAGM for 2 weeks (senescent erythrocytes) or freshly drawn and labeled intracellularly with calcein-AM and with the membrane dye PKH26 and transfused into recipient mice. Ghost erythrocytes were detected by flow cytometry ($PKH^+calcein^{lo}$). (B) Mouse organs were injected with collagenase buffer for 5 minutes after which cells and the number of

opsonized erythrocytes, or erythrocyte ghosts were incubated with PKH26 or PKH67 (1:500, 30 minutes, 37°C; Sigma-Aldrich). Standard magnetic-activated cell sorting (MACS) isolation protocols (Miltenyi Biotec, Cologne, Germany) were used to isolate monocytes from peripheral blood mononuclear cells, $CD163^+$ cells from spleen single-cell suspensions, or $F4/80^+$ cells from mouse organs. Briefly, 100 μL CD14 MACS beads were co-incubated per 5×10^7 peripheral blood mononuclear cells for 30 minutes, after which the suspension is passed over a magnetic column to isolate the monocytes. For CD163 and $F4/80^+$ cells, mouse-anti-CD163-F4/80 antibodies were conjugated to anti-mouse MACS beads. For phagocytosis assays that used total splenocytes, erythrocytes or erythrocyte ghosts were added in a 1:10 ratio and incubated in suspension for 45 minutes.

Flow assays

Erythrocyte adhesion to laminin-α5 was assessed by coating 0.5 μg laminin-511 (BioLamina) diluted in HEPES through passive adsorption on an uncoated IBIDI μ-slide VI 0.4 flow chamber (IBIDI). Erythrocytes were flowed over the substrate at 0.5 dyn/cm^2 at 37°C in $HEPES^+$. Adhesion frequency and ghost formation rate were quantified by EVOS microscopy (Thermo Fisher Scientific, Waltham, MA). Phalloidin (Thermo Fisher Scientific) was used to identify permeable ghost erythrocytes.

Isolation of dense and laminin-α5$^+$ erythrocytes and deformability measurements

Dense erythrocytes were isolated using Percoll (GE Healthcare, Little Chalfont, United Kingdom) density centrifugation. Briefly, isotonic Percoll was prepared by adding 8.1 mL 10× PBS per 100 mL Percoll. Next, Percoll buffer (26.3 g/L bovine serum albumin, 132 mM NaCl, 4.6 mM KCl, 10 mM HEPES) was used to dilute isotonic Percoll to 1.096 g/mL (80%), 1.087 g/mL (71%), 1.080 g/mL (64%), and 1.060 g/mL (40%), respectively. Percoll dilutions were stacked in a 15-mL tube, and erythrocytes isolated from the fraction denser than 1.096 g/mL Percoll were defined as dense and old erythrocytes (roughly 3% of total erythrocytes). Laminin-α5–bound cells were MACS isolated using 1 μg laminin-α5 antibody per 2×10^6 splenocytes (ab#17107; Abcam, Cambridge, United Kingdom). Anti-mouse MACS beads (Miltenyi Biotec) were then used to isolate laminin-α5 interacting cells. Peripheral monocytes were isolated by loading freshly drawn blood diluted 1:1 in PBS on Percoll with a density of 1.067 g/mL which was spun down for 20 minutes at 1000*g*. Their deformability was assessed by using an automated rheoscope and cell analyzer at a shear stress of 3 dyn/cm^2 (Pa).

Flow cytometry, in vitro ghost generation, and data analysis

Flow cytometric analysis was performed on an LSRII + HTS (BD Biosciences), and data were analyzed by FACSDiva software (BD Biosciences). In vitro ghost cells were generated by treating 1×10^9 erythrocytes with 5 mM $NaH_2PO_4 \cdot 1\ H_2O$ (pH 8) for 15 minutes at 4°C. Erythrocyte ghosts were washed by centrifugation at 20,000*g*. Experimental data were analyzed using GraphPad Prism 6 software. Figures legends provide details the on mean ± standard error of the mean (SEM) or mean ± standard deviation (SD). Significance was tested as indicated in the legends, and data were assumed to follow a normal distribution.

Results

Erythrocyte hemolysis in human spleen tissue

RPMs in the spleen help recycle iron through continuous uptake and degradation of senescent erythrocytes.[16-18] However, little is known about the mechanisms by which RPMs recognize and phagocytose senescent erythrocytes. We isolated and characterized human spleen RPMs as well as monocytes from the spleen and from circulation. Human RPMs were isolated on the basis of their autofluorescent nature and expression of CD163 (Figure 1A-B).[19] We used RNA sequencing to confirm the expression of various RPM-specific markers by these cells, in contrast to spleen- and circulation-derived monocytes. These included the RPM-specific transcription factor SpiC, the heme-degrading enzyme heme oxygenase, and the hemoglobin-haptoglobin scavenger receptor CD163 (Figure 1C; supplemental Figure 1A-B, available on the *Blood* Web site).[20,21] These findings were confirmed by quantitative polymerase chain reaction (Figure 1D). In addition, mass spectrometry revealed that these iron-recycling–related transcripts are abundantly translated in RPMs (Figure 1E). Thus, the isolated RPMs have all the characteristics that indicate their involvement in hemoglobin turnover. However, upon isolation of RPMs from human spleen tissue, we noted that only a small proportion (~3%) of RPMs were actively digesting senescent erythrocytes (Figure 1B [right panel], F). Moreover, a proportion of the phagocytosed erythrocytes was found to be largely devoid of hemoglobin although they were not fully disintegrating (Figure 1G). On the basis of a range of variables, including the number of erythrocytes cleared daily, the number of RPMs present in the spleen, the degradation rate of erythrocytes, and the differential contribution of spleen and liver to erythrocyte turnover (supplemental Table 1A), conservative estimates indicated that at least 30-fold fewer erythrophagocytic events are observed in RPMs than were anticipated. These assumptions are based on the premise that RPMs require roughly 24 hours to digest intact erythrocytes.[22,23] However, the hemoglobin-devoid erythrocytes detected in RPMs (Figure 1G) resemble another type of erythrocyte, also known as an "erythrocyte ghost" that requires only 1 to 3 hours to be degraded.[23,24] Erythrocyte ghosts form as a consequence of hemolysis and are sometimes detected in

Figure 2 (continued) transfused red blood cells (RBCs) in organs and circulation was quantified (autofluorescent$^-$PKH$^+$Hoechst$^-$ cells; n = 6). (C) Flow cytometry gating strategy used to detect labeled and transfused mouse RBCs in various organs and the circulation of recipient mice. Cells without a nucleus are depicted on the basis of Hoechst staining. Particularly in the spleen, the calcein signal was partially lost and PKH signal was retained. The top left histogram depicts unlabeled erythrocytes and the bottom left histogram depicts the labeled erythrocytes. In the top row, the 5 columns on the right depict representative histograms of nontransfused mice, and the lower 5 columns depict transfused mice. (D) Quantification of erythrocyte ghosts in the organs and circulation of transfused mice. Ghosts were defined as the fraction of cells that are autofluorescent$^-$PKH$^+$Hoechst$^-$calcein^{lo} (n = 6). (E) Imaging flow cytometric analysis of ghost formation in the spleen of a transfused mouse. The top panel indicates intact erythrocytes (PKH$^+$calcein$^+$) and the bottom panel depicts erythrocyte ghosts (PKH$^+$calcein$^-$). White lines mark cropping lines for each image because the output files were too large. (F) Live imaging of mouse spleen by 2-photon microscopy 2 hours after erythrocyte transfusion. Arrows mark PKH$^+$calcein$^+$ cells that become single positive roughly 2 hours after transfusion (lower right panel). (G-H) Hemopexin and haptoglobin concentrations in mouse organ and circulation-derived plasma was determined by enzyme-linked immunosorbent assay (n = 7, mean ± SD). *$P < .05$; **$P < .01$; ***$P < .001$; ****$P < .0001$. AU, arbitrary units.

the circulation of patients suffering from hemolytic diseases such as sickle cell disease (Figure 1H). They are relatively stable permeable erythrocyte membranes (Figure 1H) that are largely devoid of hemoglobin (Figure 1I) and are difficult to detect when using conventional microscopy (Figure 1J). We performed imaging flow cytometry on erythrocytes isolated from human spleen tissue, which allowed us to identify a subset of permeable ghost erythrocytes by means of phalloidin staining in spleen cells that were absent in the circulation of healthy individuals (Figure 1K-L). These findings suggest that erythrocytes may be prone to hemolysis within human spleen tissue which could potentially explain the relatively infrequent detection of erythrophagocytic events in RPMs.

Transfusion of senescent erythrocytes in mice results in hemolysis specifically in the spleen

To study whether steady-state hemolysis gives rise to erythrocyte ghosts in spleen tissue, we performed a series of in vivo transfusion experiments in mice. We isolated fresh mouse erythrocytes and generated senescent erythrocytes by storing them in SAGM for 2 weeks at 4°C, a strategy that is often used to induce and study clearance of senescent erythrocytes in animal models.[25-27] During erythrocyte storage, erythrocyte ageing, and sickle cell disease (states in which erythrocytes are prone to sequestration from the circulation), dehydration (supplemental Figure 1C), loss of deformability (supplemental Figure 1D), and sialic acid loss (supplemental Figure 1E) are observed, which are events that strongly correlate with removal of erythrocytes from the circulation. Thus, storage of erythrocytes is a relevant model for studying erythrocyte clearance mechanisms. The fresh and stored (henceforth termed senescent erythrocytes) mouse erythrocytes were labeled intracellularly with calcein, and their membrane was labeled using PKH (Figure 2A). We verified that in vitro ghost formation results in leakage of the intracellular dye, but the extracellular membrane dye remains (supplemental Figure 2A). We transfused labeled senescent erythrocytes into mice, and 2 hours after transfusion, we isolated erythrocytes from circulation and made collagenase-liberated single-cell suspensions of both control and transfused mouse liver, spleen, kidney, and lung cells. By tracking the nonnucleated $PKH^+calcein^+$ cells, we determined that the majority of senescent erythrocytes had localized to the spleen (Figure 2B). Specifically in this organ, a large number of the $PKH^+calcein^+$ double-positive erythrocytes had become $PKH^+calcein^-$, which was especially prominent after transfusion of senescent erythrocytes (Figure 2C-D). This finding suggests that senescent erythrocytes are specifically trapped within the spleen before they become erythrocyte ghosts. Imaging flow cytometry confirmed that these $PKH^+calcein^-$ cells were erythrocyte ghosts (Figure 2E). Intravital microscopy within intact spleen tissue allowed us to visualize the transition of $PKH^+calcein^+$ erythrocytes into $PKH^+calcein^-$ ghosts (Figure 2F). Moreover, we found that concentrations of the hemoglobin and heme scavenging molecules haptoglobin and hemopexin are significantly reduced in plasma extruded from mouse spleen compared with plasma from liver and circulation under steady-state conditions (Figure 2G-H), which may indicate their continuous consumption in this organ. Taken together, these data confirm that senescent erythrocytes hemolyze in the spleen, giving rise to erythrocyte ghosts.

Erythrocyte ghosts, but not senescent erythrocytes, are targeted for phagocytosis by human RPMs

The notion that the splenic red pulp environment may be essential in facilitating erythrophagocytosis was already put forward by Gottlieb et al,[15] who noted that physiologically aged erythrocytes are phagocytosed by RPMs in vivo, but not in vitro. However, the hypothesis that the splenic architecture may drive erythrophagocytosis through hemolysis is a novel concept that has not been explored before. Thus, we first investigated the propensity of RPMs to interact with senescent and ghost erythrocytes. We co-incubated senescent erythrocytes and erythrocyte ghosts generated in vitro (Figure 3A) with RPMs from human spleen tissue. We noted that erythrocyte ghosts, in sharp contrast to intact senescent erythrocytes, were readily phagocytosed by RPMs (Figure 3B). Interestingly, this interaction was independent of complement and complement receptor 3 (Figure 3C), which are often involved in the clearance of cellular debris.[28,29] This suggests that RPMs are capable of directly recognizing and degrading ghost erythrocytes. Recently Sosale et al[30] described how cell rigidity can override CD47-SIRPα self-signaling, which may explain why ghost erythrocytes that are not easily deformable (supplemental Figure 2B) are prone to phagocytosis. In line with studies that assessed the degradation rates of ghost erythrocytes by mouse Kuppfer cells and peritoneal macrophages,[23,24] the degradation of erythrocyte ghosts by human RPMs was found to proceed significantly faster than that of intact erythrocytes that were phagocytosed through immunoglobulin G opsonization (Figure 3D). These results were also established in vivo. Transfusion of calcein- and PKH-labeled senescent erythrocytes into mice caused splenic RPMs to interact predominantly with erythrocyte ghosts (Figure 3E, $PKH^+calcein^-$ fraction). Hemolysis and phagocytosis of ghost erythrocytes again specifically occurred upon transfusion of senescent erythrocytes as determined by benzidine staining of isolated $F4/80^+$ cells from mouse spleen (Figure 3F-G). These findings further underscore the propensity of senescent erythrocytes to undergo hemolysis within the spleen, resulting in ghost cell formation, which is followed by their rapid uptake and degradation by RPMs. This phenomenon may explain the apparent discrepancy between the number of observed and anticipated erythrophagocytic events in human RPMs. Furthermore, this may also explain the necessity for the abundant expression of CD163, the hemoglobin-haptoglobin scavenger receptor, in the spleen to scavenge free hemoglobin.[19]

Exposure of laminin-α5 in human spleen tissue facilitates sequestration of senescent erythrocytes through activation of their adhesion molecules

Next, we tried to determine the mechanisms by which the splenic environment may drive hemolysis of senescent erythrocytes. The splenic red pulp architecture consists of narrow endothelial slits, which aged erythrocytes are incapable of traversing because of their stiffness, which leads to their sequestration.[9,31,32] Furthermore, activation of the adhesion molecules Lu/BCAM and CD44, specifically on aged erythrocytes, is proposed to contribute to their retention in the spleen.[10,11] On the basis of these observations, we hypothesized that mechanical or adhesion molecule–mediated trapping of erythrocytes under shear stress conditions may result in ghost cell formation. To test this phenomenon, we set up an in vitro

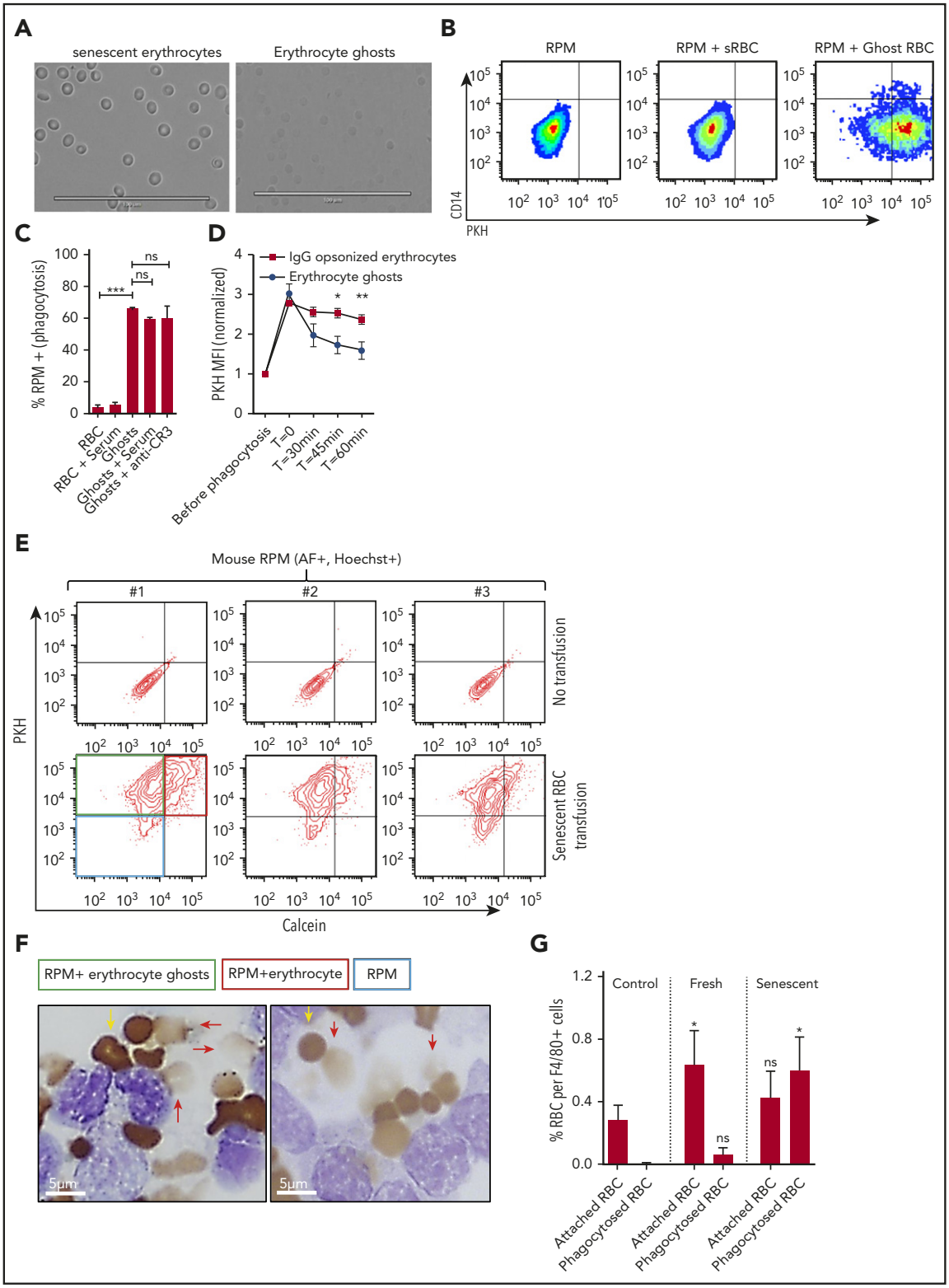

Figure 3. RPMs recognize and degrade erythrocyte ghosts in vivo and in vitro. (A) Micrograph of dense erythrocytes from healthy volunteers by density centrifugation (senescent erythrocytes, left panel) and in vitro generation of ghost erythrocytes (right panel). (B-C) Senescent erythrocytes (sRBCs) and ghost erythrocytes (ghost RBCs) were stained with PKH and coincubated with a single-cell suspension of human spleen cells for 45 minutes at 37°C, were vigorously washed, and their interaction with RPMs ($CD163^+Hoechst^+AF^+CD14^-$ subpopulation) was quantified by flow cytometry. (D) Erythrocyte and ghost breakdown rates by RPMs were quantified by measuring mean fluorescence intensity (MFI) of PKH during a time course of 60 minutes. (E) Mice received either a transfusion of PKH- and calcein-labeled senescent erythrocytes (bottom row, red quadrant) or vehicle (top row). RPMs were gated on the basis of autofluorescence and Hoechst staining. (F-G) $F4/80^+$ MACS-isolated cells from mice that received no transfusion, a fresh transfusion, or a transfusion of senescent erythrocytes were MACS isolated and subjected to benzidine staining. Attached and phagocytosed erythrocytes were quantified. Red arrows indicate phagocytosed erythrocytes and ghosts and yellow arrows indicate intact erythrocytes. Phagocytosed erythrocytes and erythrocyte ghosts (red arrows) were observed only upon transfusion of senescent erythrocytes. $*P < .05$; $**P < .01$; $***P < .001$; $****P < .0001$. Error bars indicate SD unless stated otherwise.

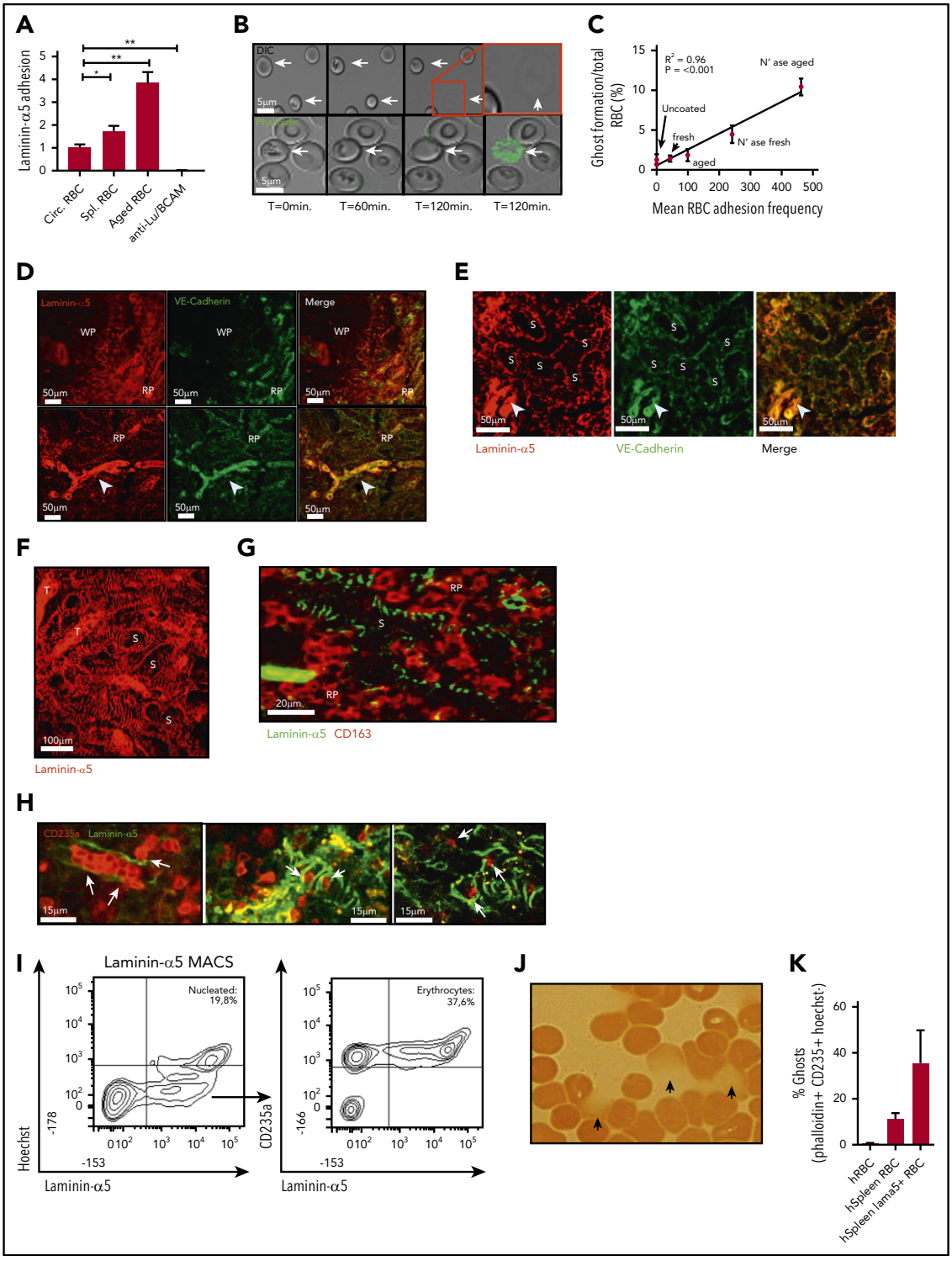

Figure 4. Adhesion of senescent erythrocytes to laminin-α5 in the human spleen drives ghost formation. (A) Laminin-α5 flow assay using control, old, and spleen-derived erythrocytes. Anti-Lu/BCAM blocking antibody was used to assess whether adhesion to laminin-α5 was Lu/BCAM dependent (n = 4-7, mean ± SEM). (B) Representative flow assay confocal micrograph depicting erythrocytes that interact with laminin-α5 for extended durations at low shear stresses of 0.5 dyn/cm^2. Erythrocyte shape abnormalities are observed after roughly 1 hour (T = 60 minutes, arrows), and ghost formation is observed after roughly 2 hours. The lower panel depicts a flow experiment in which phalloidin has been added to the flow medium. Upon ghost formation through hemolysis, the erythrocyte membrane becomes permeable, leading to intracellular F-actin staining by phalloidin. (C) Correlation between adhesion of fresh, control, and neuraminidase-treated erythrocytes to laminin-α5 and the rate at which ghost formation is observed. (D-G). Laminin-α5 localization with respect to the white pulp (WP), red pulp (RP), the RP sinus (S) CD163$^+$ cells and trabeculae (T). Continuous VE-cadherin distribution (arrowhead) was observed on protruding veins but not within the sinuses. (H) A 2-photon micrograph showing laminin-α5 distribution in the splenic sinusoids of the RP and their interaction (white arrows) with erythrocytes (glycophorin-A, CD235a) up to 100 μm deep within an intact piece of human spleen. (I) Flow cytometric gating strategy and quantification of nucleated cells that interact with laminin-α5 (Hoechst$^+$), erythrocytes (Hoechst$^-$CD235a$^+$), and other cells (Hoechst$^-$ CD235a$^-$) from human spleen. (J) Hemoglobin content of laminin-α5 MACS-isolated erythrocytes was assessed by using benzidine staining. Hemoglobin leakage was observed as indicated by the arrows. (K) Quantification of laminin-α5 positive and negative erythrocyte ghosts within human spleen tissue. *$P < .05$; **$P < .01$ (mean ± SD).

flow assay in which freshly drawn erythrocytes, aged erythrocytes derived from circulation, and spleen-derived erythrocytes were directed over a surface coated with laminin-α5, the ligand of Lu/BCAM. We confirmed that aged and spleen-derived erythrocytes adhere significantly more frequently to laminin-α5 than total circulating erythrocytes (Figure 4A) in contrast to ligands such as collagen and fibronectin (supplemental Figure 2C). Although erythrocytes that adhere to laminin-α5 initially appear intact and viable, prolonged interaction under low shear forces resulted in gradual cell shrinkage, a marked loss of biconcavity, and ultimately ghost formation on a large scale (Figure 4B). These cells were determined not to be reticulocytes because no enrichment of these cells was found by using thiazol orange stain (supplemental Figure 2E). In line with this finding, in vitro activation of Lu/BCAM through removal of membrane sialic acid[10] allowed us to establish that erythrocyte adhesion frequency directly correlates with ghost formation through hemolysis (Figure 4C). Of interest, ghost formation was not limited to adhesion to laminin-α5 but was also observed in response to adhesion to hyaluronic acid. In contrast, ghost formation was not observed when erythrocytes were flowed over collagen and fibronectin, strongly correlating with a lowered adhesion frequency (supplemental Figure 2C-D). Thus, trapping or retention of erythrocytes under shear forces induces hemolysis. Because vascular endothelium normally separates extracellular matrix (ECM) molecules such as laminin-α5 from circulating erythrocytes,[33,34] the function of receptors that recognize ECM on mature erythrocytes has remained unclear.[35-37] However, because erythrocytes within the spleen are forced through endothelial fenestrae to re-enter the circulation, we hypothesized that here, ECM proteins such as laminin-a5 may capture aged erythrocytes.[1,38] To address whether receptors that recognize ECM (such as Lu/BCAM) may contribute to their being trapped in the spleen and thereby facilitating hemolysis, we studied the distribution of laminin-α5 in this organ. We found that laminin-α5 is abundantly expressed in the red pulp (RP) of the human spleen, as opposed to the white pulp (WP) (Figure 4D). Next, we assessed the distribution of laminin-α5 in the RP sinuses, because these are the structures in which senescent erythrocytes are sequestered. Here, expression of VE-cadherin is discontinuous to allow highly deformable, but not senescent erythrocytes, to squeeze through the endothelium. We found this RP structure to be wrapped in a web-like fashion by laminin-α5 (Figure 4E-G). Thus, the localization of laminin-α5 is such that it may interact with erythrocytes entering the RP sinuses. To further address whether this is likely to occur, we performed 2-photon microscopy to image deep within human spleen tissue. We observed that erythrocytes are in close proximity to laminin-α5 within the RP sinuses (Figure 4H). To further address whether erythrocytes may interact with laminin-α5 in human spleen tissue, we isolated the cells that interact with laminin-a5 from this organ. Interestingly, we found that a substantial proportion of the laminin-α5–binding cells, next to nucleated cells, were erythrocytes (Figure 4I). Strikingly, these erythrocytes resembled senescent erythrocytes on the basis of their irregular morphology (supplemental Figure 3A), reduced cell size (supplemental Figure 3B), and decreased deformability (supplemental Figure 3C). These findings suggest that mainly senescent erythrocytes are prone to interact with laminin-α5 in human spleen tissue. As determined by benzidine staining, a substantial population of the erythrocytes that bind laminin-α5 were found to be leaking hemoglobin (Figure 4J). Furthermore, phalloidin staining confirmed that these cells were permeable erythrocyte ghosts (Figure 4K). Taken together, these data show that the ECM protein laminin-α5 within the human spleen tissue mainly interacts with senescent erythrocytes and that this is associated with ghost formation. Furthermore, the leftover erythrocyte ghosts are prone to recognition, phagocytosis, and rapid degradation by RPMs. Thus, these data indicate that hemolysis of senescent erythrocytes functions to increase the efficiency by which RPMs from the human spleen are able to recognize and degrade senescent erythrocytes. These findings can help explain the apparent discrepancy between expected and observed erythrophagocytic events in RPMs as well as the tendency of RPMs to only phagocytose senescent erythrocytes in vivo, but not in vitro, because ghost formation is likely to be a prerequisite for this process.

Discussion

In our study, we showed that adhesion of senescent erythrocytes to the ECM (mediated by adhesion molecules) in the spleen results in hemolysis before phagocytosis by RPMs. These findings explain the apparent lack of erythrophagocytic events of intact erythrocytes that are observed in RPMs from human spleen, as we and others have shown that erythrocyte ghosts are subject to far quicker degradation rates than intact erythrocytes.[23,24] This also explains why erythrophagocytosis of senescent erythrocytes is observed only in vivo, but not in vitro,[15] because the splenic architecture is required to drive hemolysis that allows for the recognition of the erythrocyte remnant by RPMs. Our data thus suggest that iron recycling is not necessarily preceded by erythrophagocytosis. Scavenging of heme from the splenic environment, rather than from internal phagolysosomes, may be a more efficient way of recycling iron, which would also explain the necessity for the high expression levels of CD163 within healthy human spleen tissue.[19] However, release of hemoglobin into the vascular space has always been regarded as a dangerous process. This is especially clear in hemoglobinopathies such as sickle cell disease, in which hemolysis is exacerbated, hemoglobin scavenger molecules are depleted, and free hemoglobin autooxidation leads to production of toxic superoxide and hydroxyl radicals that are harmful to the kidney and vasculature.[39] However, the high steady-state concentrations of plasma haptoglobin and hemopexin[40] as well as high levels of CD163 expression[19] may render the spleen especially well-suited for handling free hemoglobin. Indeed, clearing hemoglobin from 20×10^9 erythrocytes on a daily basis has been estimated to equal a total of $\sim 5 \times 10^{18}$ to 6×10^{18} hemoglobin molecules.[40] With an estimated presence of $\sim 2.8 \times 10^{19}$ haptoglobin and 1.8×10^{19} hemopexin molecules in human plasma under steady-state conditions,[40] there is ample capacity for recycling of free hemoglobin. In conclusion, our data reveal a novel mechanism by which erythrocyte sequestration and turnover is driven, also in steady state, which changes our current understanding of how iron recycling is regulated.

Acknowledgement

This work was supported by a grant from the Landsteiner Foundation for Blood Transfusion Research (LSBR1412) (T.R.L.K.).

Authorship

Contribution: T.R.L.K. designed and performed experiments, designed the figures, and wrote the manuscript; J.D. performed flow cytometry

experiments; B.N analyzed RNA sequencing data; F.P.J.M. performed imaging flow cytometry; S.Q.N. helped with cell isolation; W.F.J.v.I. and E.O. performed RNA sequencing; A.B.M. and F.P.J.v.A. performed and analyzed mass spectrometry data; M.H. and T.R. performed confocal and 2-photon experiments; P.S. and S.K.M provided mice and performed mouse experiments; M.V. performed deformability assays; and T.W.K., R.v.Z., and R.v.B. supervised and edited the manuscript.

Conflict-of-interest disclosure: The authors declare no competing financial interests.

ORCID profiles: B.N., 0000-0001-7500-5760; T.R., 0000-0003-0286-418X; S.Q.N., 0000-0001-8359-4016; W.F.J.v.I.J., 0000-0002-0421-8301; S.K.M., 0000-0003-3862-2107; T.W.K., 0000-0002-7421-3370.

Correspondence: Thomas Klei, Sanquin Bloedvoorziening, Plesmanlaan 125, 1066 CX Amsterdam, The Netherlands; e-mail: t.klei@sanquin.nl.

Footnotes

Submitted 20 February 2020; accepted 24 July 2020; prepublished online on *Blood* First Edition 10 August 2020. DOI 10.1182/blood.2020005351.

Sequencing data were deposited at the Gene Expression Omnibus (GEO) with accession number GSE121629. For other data, please e-mail the corresponding author.

The online version of this article contains a data supplement.

There is a *Blood* Commentary on this article in this issue.

The publication costs of this article were defrayed in part by page charge payment. Therefore, and solely to indicate this fact, this article is hereby marked "advertisement" in accordance with 18 USC section 1734.

REFERENCES

1. Mebius RE, Kraal G. Structure and function of the spleen. *Nat Rev Immunol*. 2005;5(8):606-616.
2. de Back DZ, Kostova EB, van Kraaij M, van den Berg TK, van Bruggen R. Of macrophages and red blood cells; a complex love story. *Front Physiol*. 2014;5:9.
3. Burger P, Hilarius-Stokman P, de Korte D, van den Berg TK, van Bruggen R. CD47 functions as a molecular switch for erythrocyte phagocytosis. *Blood*. 2012;119(23):5512-5521.
4. Seppi C, Castellana MA, Minetti G, Piccinini G, Balduini C, Brovelli A. Evidence for membrane protein oxidation during in vivo aging of human erythrocytes. *Mech Ageing Dev*. 1991;57(3):247-258.
5. Arese P, Turrini F, Schwarzer E. Band 3/complement-mediated recognition and removal of normally senescent and pathological human erythrocytes. *Cell Physiol Biochem*. 2005;16(4-6):133-146.
6. Danon D, Marikovsky Y. The aging of the red blood cell. A multifactor process. *Blood Cells*. 1988;14(1):7-18.
7. Deplaine G, Safeukui I, Jeddi F, et al. The sensing of poorly deformable red blood cells by the human spleen can be mimicked in vitro. *Blood*. 2011;117(8):e88-e95.
8. Duez J, Holleran JP, Ndour PA, et al. Mechanical clearance of red blood cells by the human spleen: Potential therapeutic applications of a biomimetic RBC filtration method. *Transfus Clin Biol*. 2015;22(3):151-157.
9. Huang S, Amaladoss A, Liu M, et al. In vivo splenic clearance correlates with in vitro deformability of red blood cells from Plasmodium yoelii-infected mice. *Infect Immun*. 2014;82(6):2532-2541.
10. Klei TRL, de Back DZ, Asif PJ, et al. Glycophorin-C sialylation regulates Lu/BCAM adhesive capacity during erythrocyte aging. *Blood Adv*. 2018;2(1):14-24.
11. Kerfoot SM, McRae K, Lam F, et al. A novel mechanism of erythrocyte capture from circulation in humans. *Exp Hematol*. 2008;36(2):111-118.
12. Bruce LJ, Ring SM, Ridgwell K, et al. Southeast Asian ovalocytic (SAO) erythrocytes have a cold sensitive cation leak: implications for in vitro studies on stored SAO red cells. *Biochim Biophys Acta*. 1999;1416(1-2):258-270.
13. Liu SC, Zhai S, Palek J, et al. Molecular defect of the band 3 protein in southeast Asian ovalocytosis. *N Engl J Med*. 1990;323(22):1530-1538.
14. Moulin PA, Baccini V. Incidental finding of 3 Southeast Asian ovalocytosis cases by attentive examination of blood smears. *Blood*. 2017;129(1):133.
15. Gottlieb Y, Topaz O, Cohen LA, et al. Physiologically aged red blood cells undergo erythrophagocytosis in vivo but not in vitro. *Haematologica*. 2012;97(7):994-1002.
16. Jandl JH, Greenberg MS, Yonemoto RH, Castle WB. Clinical determination of the sites of red cell sequestration in hemolytic anemias. *J Clin Invest*. 1956;35(8):842-867.
17. Shemin D, Rittenberg D. The life span of the human red blood cell. *J Biol Chem*. 1946;166(2):627-636.
18. Crosby WH. Normal functions of the spleen relative to red blood cells: a review. *Blood*. 1959;14(4):399-408.
19. Nagelkerke SQ, Bruggeman CW, den Haan JMM, et al. Red pulp macrophages in the human spleen are a distinct cell population with a unique expression of Fc-γ receptors. *Blood Adv*. 2018;2(8):941-953.
20. Kohyama M, Ise W, Edelson BT, et al. Role for Spi-C in the development of red pulp macrophages and splenic iron homeostasis. *Nature*. 2009;457(7227):318-321.
21. Kurotaki D, Uede T, Tamura T. Functions and development of red pulp macrophages. *Microbiol Immunol*. 2015;59(2):55-62.
22. Kondo H, Saito K, Grasso JP, Aisen P. Iron metabolism in the erythrophagocytosing Kupffer cell. *Hepatology*. 1988;8(1):32-38.
23. Loegering DJ, Commins LM, Minnear FL, Gary LA, Hill LA. Effect of Kupffer cell phagocytosis of erythrocytes and erythrocyte ghosts on susceptibility to endotoxemia and bacteremia. *Infect Immun*. 1987;55(9):2074-2080.
24. Mellman IS, Plutner H, Steinman RM, Unkeless JC, Cohn ZA. Internalization and degradation of macrophage Fc receptors during receptor-mediated phagocytosis. *J Cell Biol*. 1983;96(3):887-895.
25. Gilson CR, Kraus TS, Hod EA, et al. A novel mouse model of red blood cell storage and posttransfusion in vivo survival. *Transfusion*. 2009;49(8):1546-1553.
26. Straat M, Klei T, de Korte D, van Bruggen R, Juffermans NP. Accelerated clearance of human red blood cells in a rat transfusion model. *Intensive Care Med Exp*. 2015;3(1):27.
27. Hod EA, Arinsburg SA, Francis RO, Hendrickson JE, Zimring JC, Spitalnik SL. Use of mouse models to study the mechanisms and consequences of RBC clearance. *Vox Sang*. 2010;99(2):99-111.
28. Cresci GA, Allende D, McMullen MR, Nagy LE. Alternative complement pathway component Factor D contributes to efficient clearance of tissue debris following acute CCl_4-induced injury. *Mol Immunol*. 2015;64(1):9-17.
29. Noris M, Remuzzi G. Overview of complement activation and regulation. *Semin Nephrol*. 2013;33(6):479-492.
30. Sosale NG, Rouhiparkouhi T, Bradshaw AM, Dimova R, Lipowsky R, Discher DE. Cell rigidity and shape override CD47's "self"-signaling in phagocytosis by hyperactivating myosin-II. *Blood*. 2015;125(3):542-552.
31. Klausner MA, Hirsch LJ, Leblond PF, Chamberlain JK, Klemperer MR, Segel GB. Contrasting splenic mechanisms in the blood clearance of red blood cells and colloidal particles. *Blood*. 1975;46(6):965-976.
32. Pivkin IV, Peng Z, Karniadakis GE, Buffet PA, Dao M, Suresh S. Biomechanics of red blood cells in human spleen and consequences for physiology and disease. *Proc Natl Acad Sci U S A*. 2016;113(28):7804-7809.
33. Hayden MR, Sowers JR, Tyagi SC. The central role of vascular extracellular matrix and basement membrane remodeling in metabolic syndrome and type 2 diabetes: the matrix preloaded. *Cardiovasc Diabetol*. 2005;4(1):9.
34. Kalluri R. Basement membranes: structure, assembly and role in tumour angiogenesis. *Nat Rev Cancer*. 2003;3(6):422-433.

35. Telen MJ. Red blood cell surface adhesion molecules: their possible roles in normal human physiology and disease. *Semin Hematol*. 2000;37(2):130-142.

36. Parsons SF, Spring FA, Chasis JA, Anstee DJ. Erythroid cell adhesion molecules Lutheran and LW in health and disease. *Best Pract Res Clin Haematol*. 1999;12(4):729-745.

37. Kikkawa Y, Miner JH. Review: Lutheran/B-CAM: a laminin receptor on red blood cells and in various tissues. *Connect Tissue Res*. 2005;46(4-5):193-199.

38. Buffet PA, Safeukui I, Milon G, Mercereau-Puijalon O, David PH. Retention of erythrocytes in the spleen: a double-edged process in human malaria. *Curr Opin Hematol*. 2009;16(3):157-164.

39. Rifkind JM, Mohanty JG, Nagababu E. The pathophysiology of extracellular hemoglobin associated with enhanced oxidative reactions. *Front Physiol*. 2015;5:500.

40. Smith A, McCulloh RJ. Hemopexin and haptoglobin: allies against heme toxicity from hemoglobin not contenders. *Front Physiol*. 2015;6:187.